Virology 535 (2019) 162–170

Contents lists available at ScienceDirect

Virology

journal homepage: www.elsevier.com/locate/virology

Host microRNA miR-1307 suppresses foot-and-mouth disease virus replication by promoting VP3 degradation and enhancing innate immune response

Linlin Qi[a,b,1], Kailing Wang[a,1], Haotai Chen[a,b], Xinsheng Liu[a,b], Jianliang Lv[a,b], Shitong Hou[a], Yongguang Zhang[a,b,**], Yuefeng Sun[a,b,*]

[a] State Key Laboratory of Veterinary Etiological Biology, National Foot and Mouth Diseases Reference Laboratory, Key Laboratory of Animal Virology of Ministry of Agriculture, Lanzhou Veterinary Research Institute, Chinese Academy of Agricultural Sciences, Lanzhou, 730046, PR China
[b] Jiangsu Co-innovation Center for Prevention and Control of Important Animal Infectious Diseases and Zoonoses, Yangzhou University, Yangzhou, 225009, PR China

ARTICLE INFO

Keywords:
Foot-and-mouth disease virus
miR-1307
VP3
Immune response

ABSTRACT

MicroRNAs (miRNAs) play important regulatory roles during interactions between virus pathogens and host cells, but whether and how they work in the case of foot-and-mouth disease virus (FMDV) is less understood. Based on a microarray-based miRNA profiling in the porcine kidney cell line PK-15, we identified 36 differentially expressed host miRNAs at the early stage of FMDV infection, among which miR-1307 was significantly induced. Functional characterization demonstrated that miR-1307 attenuated FMDV replication. Further experiments proved that miR-1307 specifically promoted the degradation of the viral structural protein VP3 indirectly through proteasome pathway. Moreover, innate immune signaling was activated and expression of immune responsive genes was significantly enhanced in the miR-1307-overexpressing clones. Together, our data demonstrated that miR-1307 suppresses FMDV replication by destabilizing VP3 and enhancing host immune response. Importantly, subcutaneous injection of miR-1307 agomir delayed the FMDV-induced lethality in suckling mice, exhibiting its therapeutic potential to control foot-and-mouth disease (FMD).

1. Introduction

Foot-and-mouth disease virus (FMDV) is the etiological agent of foot-and-mouth disease (FMD), economically the most important animal disease affecting cloven-hoofed animals, ranking first in the A list of infectious animal diseases, according to the Office International des Epizooties (Bachrach, 1968; Sobrino et al., 2001). Due to its rapid evolution, seven main serotypes (A, O, C, Asia1, South African Territories (SAT) 1, SAT2, and SAT3) exist in the world (Domingo et al., 2005). FMDV belongs to the *aphthovirus* genus of the family *Picornaviridae*. Its genome is a positive single-strand RNA of about 8500 nucleotides containing a single open reading frame (ORF) that is translated into a polyprotein, which is further processed into four structural proteins (VP1, VP2, VP3, and VP4), and 10 non-structural proteins (NSPs) (Lpro, 2A, 2B, 2C, 3A, 3B1–3, 3Cpro, and 3Dpol) by the viral proteases Lpro and 3Cpro (Domingo et al., 2002; Gao et al., 2016). During FMDV infection, the replicative intermediate double-stranded RNA (dsRNA) can be perceived by host cytoplasmic virus sensors melanoma differentiation-associated gene 5 (MDA5) and retinoic acid-inducible gene-I (RIG-I) to trigger a signaling cascade to stimulate the expression of type-I interferon (IFN) and proinflammatory cytokines through nuclear transcription factor kappa B (NF-κB) and IFN-regulatory factors 3 and 7 (IRF 3/7) activation, thus establishing an antiviral state within infected cells (Deddouche et al., 2014; Feng et al., 2012; Zhu et al., 2016). On the other side, FMDV also evolves sophisticated strategies to counteract the host immune responses to facilitate its replication (de Los Santos et al., 2007; Du et al., 2014; Guarne et al., 1998; Wang et al., 2012a; Wang et al., 2011). To date, the molecular mechanisms underlying the FMDV-host interaction is still less understood.

MicroRNAs (miRNAs) are ~21-nucleotide-long non-coding RNAs (ncRNAs) that regulate genes expression post-transcriptionally. Typically, they are transcribed by RNA polymerase II from miRNAs genes to produce primary transcripts (pri-miRNAs) with stem-loop

* Corresponding author. Lanzhou Veterinary Research Institute, Chinese Academy of Agricultural Sciences, Lanzhou 730046, PR China.
** Corresponding author. Lanzhou Veterinary Research Institute, Chinese Academy of Agricultural Sciences, Lanzhou 730046, PR China.
E-mail addresses: zhangyongguang@caas.cn (Y. Zhang), sunyuefeng@caas.cn (Y. Sun).
[1] These authors made equal contribution to the work.

https://doi.org/10.1016/j.virol.2019.07.009
Received 22 April 2019; Received in revised form 3 July 2019; Accepted 8 July 2019
Available online 09 July 2019
0042-6822/

structures, which are processed by Drosha-containing complex into ~70-nucleotide precursor miRNAs (pre-miRNAs). The pre-miRNAs are exported to cytoplasm where they are further processed by Dicer to ~21-bp miRNA/miRNA* duplexes. The mature miRNAs (one strand of the duplex) are loaded into Argonaute proteins (mainly AGO2) to form the miRNA-induced silencing complex (miRISC) (Krol et al., 2010). As part of the complex, the mature miRNAs base-pair to target mRNAs containing complementary sequences, resulting in translational blockade or mRNA degradation (Huntzinger and Izaurralde, 2011). Accumulating evidences have demonstrated that cellular miRNAs play important regulatory roles during interaction of various viruses with host cells and manipulation of miRNAs has shown prospects for antiviral therapeutic application (Browne et al., 2005; Bruscella et al., 2017; Laqtom and Buck, 2011; Tsunetsugu-Yokota and Yamamoto, 2010). In the case of FMDV, multiple artificial miRNAs targeting viral 3Dpol or internal ribosome entry site had been designed to efficiently inhibit FMDV replication (Chang et al., 2013; Du et al., 2011). However, whether and how endogenous host miRNAs play regulatory roles during FMDV-host interaction is still less studied. It has been shown that 244 miRNAs were differentially expressed after FMDV infection in porcine kidney cell line (PK-15), suggesting possible regulatory functions during this process, but their functional meaning awaits further study (Zhang et al., 2014). Until recently, host miR-203a was shown to be antagonistic to the FMDV progression (Gutkoska et al., 2017), which might be only a tip of the iceberg among the sophisticated miRNAs regulatory network.

Here we successfully identified a host miRNA miR-1307 whose expression was rapidly induced in porcine cell lines challenged with FMDV. We further demonstrated that miR-1307 attenuated FMDV replication by destabilizing the viral structural protein VP3 and enhancing the host innate immune response. Moreover, injection of miR-1307 agomir significantly delayed the FMDV-induced death in suckling mice, indicating the therapeutic potential for FMD control of this natural endogenous miRNA.

2. Materials and methods

2.1. Cell lines and viruses

Porcine kidney cells PK-15, IBRS-2, and baby hamster kidney cells BHK-21 were cultured in Dulbecco's modified Eagle's medium (DMEM, Gibco) supplemented with 10% fetal bovine serum (FBS, Gibco) and 1% penicillin-streptomycin (Invitrogen). All cells were maintained at 37 °C with 5% CO_2 in a humidified incubator.

FMDV type O strain O/BY/CHA/2010 was stored at OIE/National Foot-and-Mouth Disease Reference Laboratory (Lanzhou, Gansu, PR China), and was used for viral challenge in this research. The viruses were propagated in BHK-21 cells. The virus titer was determined by Tissue Culture Infective Dose ($TCID_{50}$) assay using the Reed-Muench method. All the virus-related experiments were conducted in the Biosafety Level-3 (BSL-3) Laboratory of Lanzhou Veterinary Research Institute following the standard protocols and biosafety regulations provided by the Institutional Biosafety Committee.

2.2. FMDV infection

Cells were cultured in 60-mm dishes to reach an approximate 90% confluence (3×10^6). The medium were aspirated and the cells were washed once with 3 ml of FBS-free DMEM. FMDV stock at $TCID_{50}$ of 1×10^{-8}/ml were diluted in FBS-free DMEM medium to obtain the indicated multiplicity of infection (MOI). 1 ml of the diluted virus solutions were applied to each dish. Cells were then maintained in 37 °C incubator for 1 h (h). After that, the virus solutions were aspirated, the cells were washed again with FBS-free DMEM, and 3 ml of FBS-free DMEM was added to each dish for further incubation at normal conditions.

2.3. MiRNA microarray

PK-15 cells were either mock-treated or infected with FMDV (MOI = 1). At 2 h post infection (hpi), cells were collected and sent to CapitalBio Technology (Beijing, China) for Affymetrix miRNA array analysis (miRNA-4_0) following the standard protocol. The original data were collected with Affymetrix AGCC software and were further normalized and analyzed with Affymetrix Expression Console. Those with fold change ≥ 2 or ≤ 0.5 were selected as the differentially expressed miRNAs.

2.4. MiRNA reagents, plasmids and transfections

MiR-1307 mimics, inhibitors, agomir, scrambled negative-control (NC) and overexpression plasmid (pmiR-1307) were all purchased from GenePharma Co., Ltd (Shanghai, China). Especially, the miR-1307 agomir and the corresponding NC used in mice experiment were chemically modified to increase their stability *in vivo* in experimental animals.

For construction of pFLAG-VP1 and pFLAG-VP3, the PCR fragments of VP1 and VP3 were amplified from viral cDNA and were subsequently cloned into pXJ-40 vector using restriction enzyme ligation. For the other plasmids expressing different FLAG-tagged viral proteins, the construction process is similar except the backbone plasmid is changed to pCMV-3Tag-1. To test the possible miR-1307 targets, VP3 coding sequences and fragments covering the predicted target sites were amplified and ligated into pmirGLO vector, after the coding sequence of firefly luciferase (LUC). The primers used for plasmid construction are listed in Table S1.

Transfections were performed using Lipofectamine 2000 reagent (Invitrogen) following the manufacturer's instructions. To obtain the cell lines stably overexpressing miR-1307, PK-15 cells were transfected with pmiR-1307 plasmid, and single cell clones were picked using cloning-ring anchoring method after blasticidin selection and serial dilutions.

2.5. MiRNAs extraction and quantification

MiRNAs were extracted from cultured cells or tissues using mirVana miRNA Isolation Kit (Invitrogen, AM1560). Reverse transcription-quantitative real-time PCR (RT-qPCR) was used to quantify miR-1307. Briefly, 500 ng of the enriched miRNAs were polyadenylated by poly(A) polymerase and reverse transcribed into cDNA using oligo-dT primers containing a 3′ degenerate anchor and a universal tag sequence on the 5′ end using miScript II RT kit (Qiagen, 218161). Quantitative amplification of miR-1307 was performed with miR-1307-specific primer and a universal reverse primer provided in miScript SYBR Green PCR kit (Qiagen, 218073). The relative expression of miR-1307 was normalized to the internal control miR-16 (Li et al., 2012). The statistical significance was evaluated by Student's *t*-test. The primers used are listed in Table S1.

2.6. Quantitative real-time PCR

To quantify viruses in cell cultures, the whole cell cultures were lysed by three rounds of freeze-thaw. After centrifugation at 6000 revolutions per minute (rpm) for 5 min (min), 350 μl of supernatants were used for RNA extraction. To test genes expression within cells, about 3×10^6 cells were pelleted for RNA preparation. Total RNA was prepared using RNeasy Mini Kit (Qiagen, 74106) following the standard protocol and cDNA was synthesized using the iScript cDNA Synthesis kit (BioRad, 1708890). Quantitative real-time PCR (qPCR) was performed with either SYBR Green qPCR SuperMix (Takara) or TaqMan Universal PCR Master Mix (ABI) using MX3000P qPCR Machine (Agilent Technologies). For virus quantification in cell cultures, same volumes of cell lysates (350 μl), total RNA and cDNA were used for

Table 1
Differentially expressed miRNAs in PK-15 cells upon FMDV infection identified by Affymetrix miRNA array.

miRNAs	Probeset ID	Accession	Mock	FMDV	Fold change
ssc-miR-7139-3p	20526804	MIMAT0028154	5.6917	21.91415	3.8502
ssc-miR-210	20509099	MIMAT0007761	800.18	2794.676	3.4925
ssc-miR-769-3p	20514338	MIMAT0013958	14.348	44.60642	3.109
ssc-miR-30a-5p	20511623	MIMAT0010193	57.63	176.7659	3.0673
ssc-miR-139-3p	20503082	MIMAT0022921	100.56	280.5285	2.7897
ssc-miR-7134-5p	20526793	MIMAT0028143	5.2741	14.50506	2.7502
ssc-miR-2411	20524931	MIMAT0025389	85.833	235.8495	2.7478
ssc-miR-1307	20514309	MIMAT0013936	349.48	814.8292	2.3316
ssc-miR-339-3p	20514313	MIMAT0017381	6.2533	13.23066	2.1158
ssc-miR-423-5p	20514245	MIMAT0013880	458.25	957.6639	2.0898
ssc-miR-378	20514231	MIMAT0013868	1598.4	3211.683	2.0094
ssc-miR-140-3p	20503065	MIMAT0006786	371.98	746.6669	2.0073
ssc-miR-7137-3p	20526800	MIMAT0028150	6.8262	3.381752	0.4954
ssc-miR-202-3p	20514326	MIMAT0022956	6.1481	2.967315	0.4826
ssc-let-7e	20514229	MIMAT0013866	890.47	417.2227	0.4685
ssc-miR-151-3p	20514248	MIMAT0013883	75.493	35.09659	0.4649
ssc-miR-192	20514279	MIMAT0013910	21.51	9.954617	0.4628
ssc-miR-132	20524904	MIMAT0025361	7.7377	3.461947	0.4474
ssc-miR-195	20514301	MIMAT0013928	5.7876	2.551689	0.4409
ssc-miR-196b-5p	20514294	MIMAT0013923	9.7079	4.161655	0.4287
ssc-miR-196b	20524912	MIMAT0025369	9.7079	4.161655	0.4287
ssc-miR-219	20520339	MIMAT0020590	7.3903	3.13092	0.4236
ssc-miR-331-5p	20514302	MIMAT0013929	9.4251	3.83894	0.4073
ssc-miR-28-5p	20503056	MIMAT0002136	87.476	34.27417	0.3918
ssc-miR-29b	20503058	MIMAT0002137	6.8864	2.630129	0.3819
ssc-miR-128	20503079	MIMAT0002157	34.155	11.77439	0.3447
ssc-miR-7142-5p	20526809	MIMAT0028159	8.2818	2.764031	0.3337
ssc-miR-181b	20503045	MIMAT0002126	35.847	10.90562	0.3042
ssc-miR-138	20524906	MIMAT0025363	14.337	4.035808	0.2815
ssc-miR-4334-5p	20517775	MIMAT0017966	140.66	37.33155	0.2654
ssc-miR-155-5p	20517761	MIMAT0022959	72.553	16.82017	0.2318
ssc-miR-335	20514334	MIMAT0013955	39.38	7.832938	0.1989
ssc-miR-421-3p	20517782	MIMAT0022962	20.068	3.838375	0.1913
ssc-miR-152	20514253	MIMAT0013887	78.824	13.75567	0.1745
ssc-miR-28-3p	20503057	MIMAT0015211	17.847	2.967902	0.1663
ssc-miR-484	20517787	MIMAT0017974	21.859	3.180842	0.1455

downstream analysis to ensure comparability among samples. TaqMan method targeting 3D or SYBR Green method targeting VP1 was used to quantify FMDV RNA level. To evaluate genes expression, qPCR was performed using SYBR Green qPCR SuperMix (Takara) with gene-specific primers. β-actin or GAPDH was used as the internal control. The relative expression of specific gene was normalized to the internal control using $2^{-\Delta\Delta CT}$ method. The statistical significance was evaluated by Student's *t*-test. The primers for immune-responsive genes have been reported previously (Wang et al., 2012a). All the primers used are listed in Table S1.

2.7. Western blotting

Protein extraction and Western blotting were done according to standard protocols. Briefly, cells were lysed in RIPA Lysis Buffer (Pierce) supplemented with protease inhibitor cocktail (Roche). Protein concentration was determined using BCA Protein Assay Kit (Pierce). Samples were separated by sodium dodecyl sulfate (SDS)-polyacrylamide gel electrophoresis, and transferred to polyvinylidene fluoride membranes (Millipore). The primary antibodies used in this study include: mouse monoclonal *anti*-β-actin antibody (Sigma), rabbit polyclonal anti-FLAG antibody (Sigma), *anti-p*-TBK1 and *anti-p*-IRF3 antibody from RIG-I Pathway Antibody Sampler Kit (Cell Signaling), *anti*-p-p65/RelA antibody from NF-κB Pathway Sampler Kit (Cell Signaling), and self-made rabbit polyclonal *anti*-VP1 antibody (Zhu et al., 2016). Horseradish peroxidase-conjugated secondary antibodies were from Sigma. Protein bands were finally visualized by addition of SuperSignal West Pico Chemiluminescent Substrate (Thermo).

2.8. Luciferase reporter assay

BHK-21 cells were seeded in 24-well plates and were co-transfected with 200 ng of luciferase reporter plasmid and 20 pmol of miR-1307 mimics or NC using Lipofectamine 2000 reagent (Invitrogen). Twenty-four hours after transfection, firefly and Renilla luciferase activities were sequentially measured using the Dual-Glo Luciferase assay system (Promega). Relative luciferase activities were calculated as the ratio of firefly/Renilla luminescence intensity. The experiments were performed in triplicates and statistical significance was evaluated by Student's *t*-test.

2.9. MTT assay

MTT [3-(4,5-dimethylthiazol-2-yl)-diphenyl tetrazolium bromide] assay was performed as previously described (Sun et al., 2014). Briefly, Cells were seeded into 96-well plates. To measure the cell viability at specific time points, MTT reagent was added to each well with a final concentration of 0.5 mg/ml and incubated for 3 h. After removing the medium, 100 μl of DMSO was added, and the absorption at 595 nm was determined with a Varioskan™ LUX multimode microplate reader (Thermo).

2.10. Viral challenge assay in suckling mice

FMDV (O/BY/CHA/2010) used for infecting mice had been adapted in suckling mice (Balb/c) for several generations. The 50% lethal dose (LD_{50}) was determined by the Reed-Muench method. Viral challenge assay in suckling mice was performed according to the previously described method with slight modifications (Chen et al., 2004). The 3-

day-old suckling mice were subcutaneously injected in the neck with 0.6 optical density (OD) of miR-1307 agomir or NC dissolved in 100 μl of DEPC-treated dH_2O. One hour later, the suckling mice were challenged with 100 LD_{50} of FMDV diluted in 100 μl of phosphate buffered saline (PBS) by subcutaneous injection into the adjacent site. At 12 hpi, miR-1307 agomir or NC was injected again with the same method. The mice were then monitored for death every 2 h to calculate the survival rate.

3. Results

3.1. Expression of miR-1307 is stimulated after FMDV infection

In order to identify the differentially expressed miRNAs during the early stage of FMDV infection, we performed a microarray-based miRNAs profiling experiment in porcine kidney cell line PK-15 after infection for 2 h with an O-type FMDV strain (O/BY/CHA/2010) epidemic in China. As shown in Table 1, there were 36 miRNAs identified, including 12 that were upregulated and 24 downregulated upon FMDV infection. Based on that experiment, several differentially-expressed miRNAs were selected to confirm the reliability of the microarray results using RT-qPCR (Fig. S1). Since miR-1307 shows the highest induction in the RT-qPCR results, we chose it for further investigation. As we can see in Fig. 1A, the expression level of miR-1307 in FMDV-infected PK-15 cells was more than 10-fold higher than that in the mock treatment at 1 hpi, and increased further to a maximum of 20-fold at 2 hpi. The induction of miR-1307 upon FMDV infection can also be confirmed in another porcine cell line IBRS-2, with a greatest induction fold detected at 1 hpi (Fig. 1B). The rapid and drastic induction of miR-1307 upon FMDV infection suggested it might play important regulatory roles during this process.

3.2. Transfection of miR-1307 mimics or inhibitors affects FMDV replication

To evaluate the possible effects of miR-1307 on FMDV replication, we synthesized miR-1307 mimics and the corresponding NC, and transfected them into PK-15 cells. Twenty-four hours after transfection, cells were infected with FMDV at an MOI of 1 and were sampled for analysis at the different time points. As shown in Fig. 2A, the expression level of FMDV RNA was significantly reduced in cells transfected with miR-1307 mimics comparing with NC. The inhibitory effects became more obvious later at 8 hpi and 12 hpi. To exclude the possibility that miR-1307 mimics alter the cell viability, MTT assay was performed after transfection and no significant change was observed over time (Fig. S2). In comparison, we also performed a similar experiment with miR-1307 inhibitors and NC. The result showed that transfection of its inhibitors slightly increased the viral RNA abundance at the early stage of infection (Fig. 2B). Collectively, these data indicate that miR-1307 inhibits FMDV replication.

3.3. Overexpression of miR-1307 strongly suppresses FMDV replication

Transfection efficiency of miR-1307 mimics in PK-15 cells may underestimate its inhibitory effects on FMDV replication. To unbiasedly evaluate its effects, we established PK-15 cell clones stably overexpressing miR-1307. After transformation with pmiR-1307, several single clones were picked and further characterized, and two independent clones (miR-1307-11 and miR-1307-12) were finally obtained, in which expression of miR-1307 was significantly upregulated compared with control clone (Fig. S3). MTT assay was performed in the selected cell clones to exclude the possible effects on cell viability (Fig. S4). After that, we performed viral challenge assay (MOI = 1) to evaluate the effects of miR-1307 overexpression on FMDV replication. RT-qPCR results showed that FMDV RNA expression level was drastically reduced in the two clones comparing with NC at 8 hpi (Fig. 3A), and similar result was obtained from western blotting that showed the obvious reduction of the viral protein VP1 (Fig. 3B). Consistently, virus titer was also greatly decreased in these two clones at 12 hpi after challenged with 5 MOI of FMDV (Fig. 3C). Together, these data strongly proved that FMDV replication was attenuated in the miR-1307-overexpressing clones. To compare its inhibitory effects at different MOI, we chose miR-1307-12 clone for FMDV infection assay at different MOI, and the viral RNA expression levels were then quantified. The results indicated that the suppressive effects were more obvious at the higher MOI (Fig. 3D).

3.4. MiR-1307 specifically promotes the protein degradation of VP3 through proteasome pathway

Host miRNAs can inhibit viral replication through targeting viral genome or suppressing proviral host factors (Bruscella et al., 2017; Tsunetsugu-Yokota and Yamamoto, 2010). To first test whether miR-1307 has repressive effects on FMDV proteins expression, we fused different viral protein-coding regions with FLAG tag and co-transfected the resulting constructs together with miR-1307 mimics or NC into baby hamster kidney cell line BHK-21, which is widely used for FMDV research and has higher transfection efficiency. Western blotting results demonstrated that transfection of miR-1307 mimics specifically reduced the expression of the viral capsid protein VP3 from the FLAG-tagged constructs, but did not have any significant effects on the other viral proteins except Lpro and 3B that did not express well and could not be detected in our system (Fig. 4A). To test whether miR-1307 directly targets VP3, we cloned the VP3-coding sequences into the pmirGLO vector for luciferase reporter assay, which will produce LUC-VP3 fusion mRNA but only LUC in the translated protein. As shown in Fig. 4B, transfection of miR-1307 mimics did not show any significant effects on the relative luciferase activity, indicating that miR-1307 does

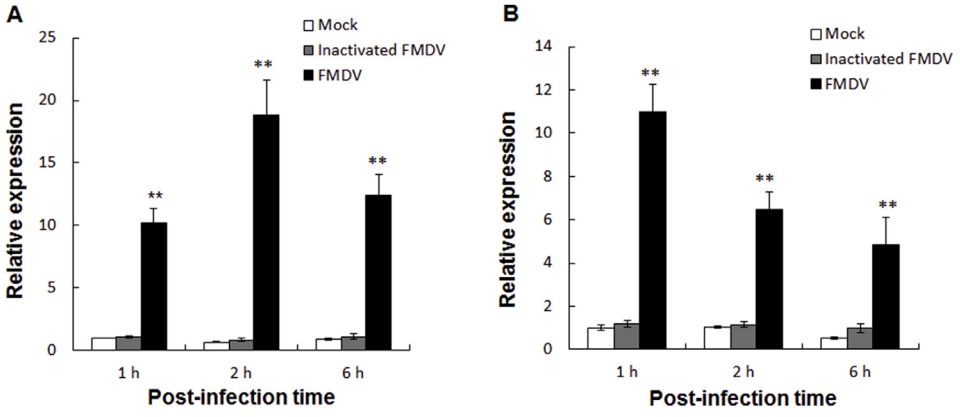

Fig. 1. FMDV infection upregulates the expression of miR-1307.
(A) and **(B)** Expression of miR-1307 in FMDV-infected porcine PK-15 (A) and IBRS-2 (B) cells. Cells were mock-treated or challenged with FMDV at 1 MOI. UV-inactivated FMDV was also used as a control. At the indicated post-infection time, expression level of miR-1307 was quantified by RT-qPCR, using miR-16 as the internal control. Data are representative of at least two independent experiments, with each determination performed in triplicates. Error bars represent standard deviation (SD). Asterisks indicate significant differences, according to Student's *t*-test, $^{**}P < 0.01$.

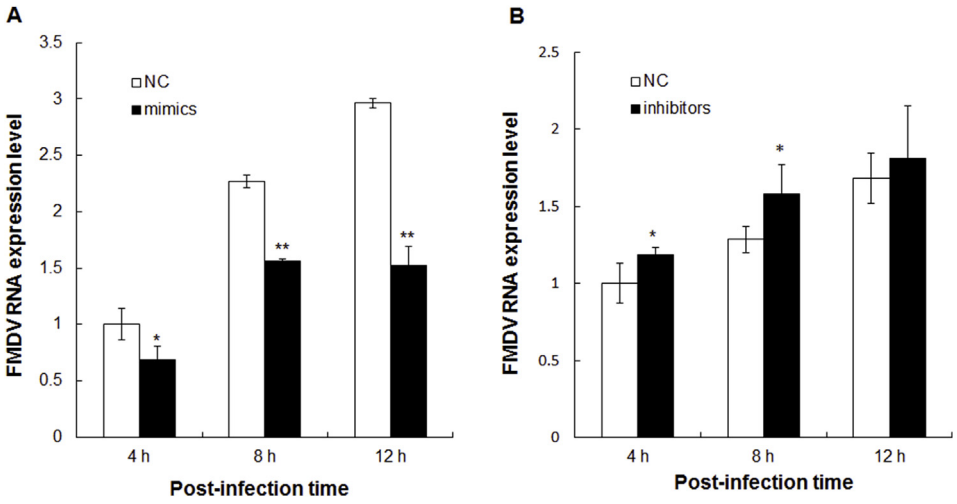

Fig. 2. Transfection of miR-1307 mimics or inhibitors affects FMDV replication.
(A) Transfection of miR-1307 mimics inhibits FMDV replication. **(B)** Transfection of miR-1307 inhibitors accelerates FMDV replication. PK-15 cells were transfected with synthetic miR-1307 mimics, inhibitors or scrambled negative-control (NC). Twenty-four hours after transfection, cells were challenged with FMDV (MOI = 1). At the indicated time points, total RNA was extracted from the equal volumes of cell culture and the FMDV RNA expression level was quantified by RT-qPCR using TaqMan method targeting 3D. Results shown are representative of three independent experiments, with each determination performed in triplicates. Bars represent SD of the mean. Asterisks indicate significant differences, according to Student's *t*-test, *, $p < 0.05$; **, $p < 0.01$.

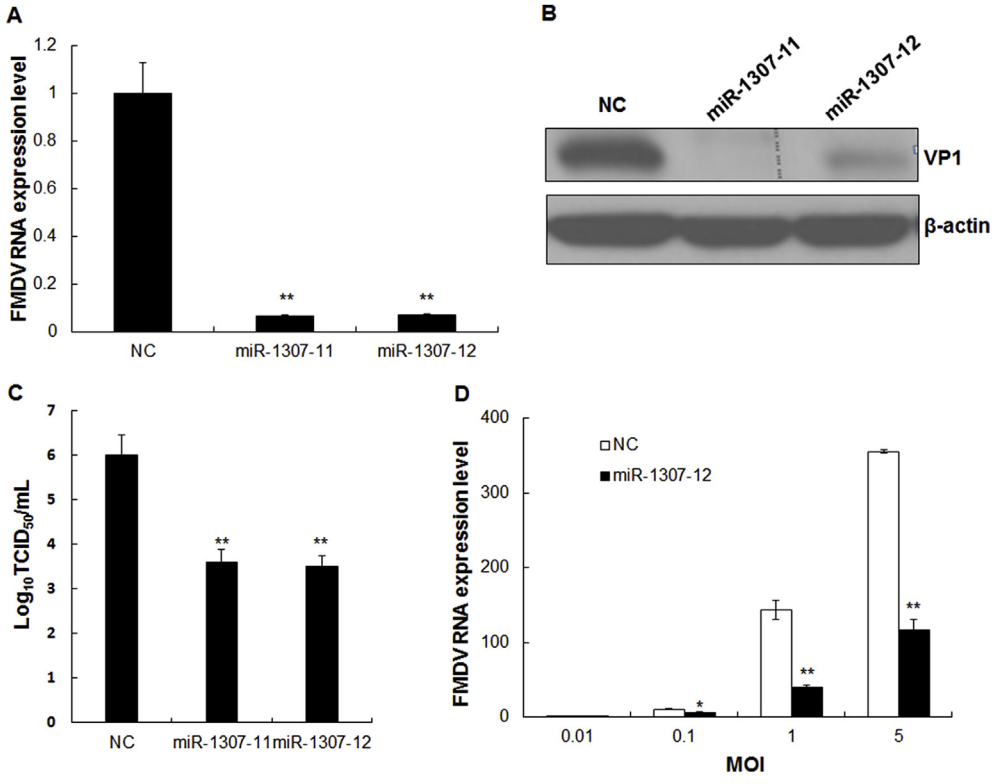

Fig. 3. Overexpression of miR-1307 suppresses FMDV replication.
(A) FMDV growth was inhibited in PK-15 cell clones stably overexpressing miR-1307 shown by RT-qPCR. Two independent PK-15 cell clones overexpressing miR-1307 and a control cell clone transformed with negative control plasmid (NC) were infected with FMDV at 1 MOI. At 8 hpi, TaqMan-based RT-qPCR targeting 3D was performed with equal volumes of cell lysates to measure FMDV RNA expression level. Asterisks indicate significant differences, according to Student's *t*-test, **, $p < 0.01$.
(B) FMDV replication was suppressed in miR-1307-overexpressing cell clones shown by western blotting. Cells were challenged and sampled at the same time point as in (A) for protein extraction and western blotting using an antibody against VP1. β-actin was used as the internal control. The experiment was repeated three times with similar results.
(C) FMDV replication was suppressed in miR-1307-overexpressing cell clones shown by virus titers. FMDV titers were measured using $TCID_{50}$ method after cells were infected with FMDV (MOI = 5) for 12 h. Shown are means ± SD from triplicate assays. ** indicates significant differences at $p < 0.01$ according to Student's *t*-test
(D) FMDV RNA expression level was reduced in miR-1307-12 after infection with FMDV at different MOI. Cells were challenged with FMDV at the indicated MOI and sampled at 12 hpi for RT-qPCR analysis. Results shown are representative of three independent experiments. Asterisks indicate significant differences, according to Student's *t*-test, *, $p < 0.05$; **, $p < 0.01$.

not target VP3 directly at RNA level. Hence, we speculated that the reductive effect on VP3 might occur at protein level. To determine whether the proteasome pathway plays roles in miR-1307-induced reduction of VP3, the proteasome inhibitor MG132 was used. The result showed that application of MG132 completely abolished the reductive effect of miR-1307 on VP3 (Fig. 4C), demonstrating that miR-1307 promotes the VP3 degradation through the proteasome pathway.

3.5. MiR-1307 enhances the innate immune response

Viral RNA can be perceived by the host cytoplasmic sensors to activate the innate immune signaling and finally stimulate the production of type-I IFNs and then the expression of IFN-stimulated genes (ISGs) (Kawai and Akira, 2006). To test the possible effects of miR-1307 on the host innate immune response, we challenged the NC and miR-1307-overexpressing cell clones described above with FMDV and analyzed the expression level of IFN-β and several ISGs, including ISG54, 2′,5′-oligoadenylate synthetase (2′,5′-OAS), IFN-inducible protein 10 (IP-10, also known as CXCL10) and regulated upon activation, normal T-cell-expressed and -secreted (RANTES, also known as CCL5), which were reported to be FMDV-inducible and necessary for the antiviral immunity against FMDV (Wang et al., 2012a). As shown in Fig. 5, in the mock-treated groups, all of these genes showed higher expression level in the overexpression cell clones comparing with those in NC, indicating miR-1307 pre-activated the immune response. After FMDV infection for 12 h, the expression level of most of these genes were still significantly higher in the overexpression cell clones except RANTES whose expression level was comparable between NC and the

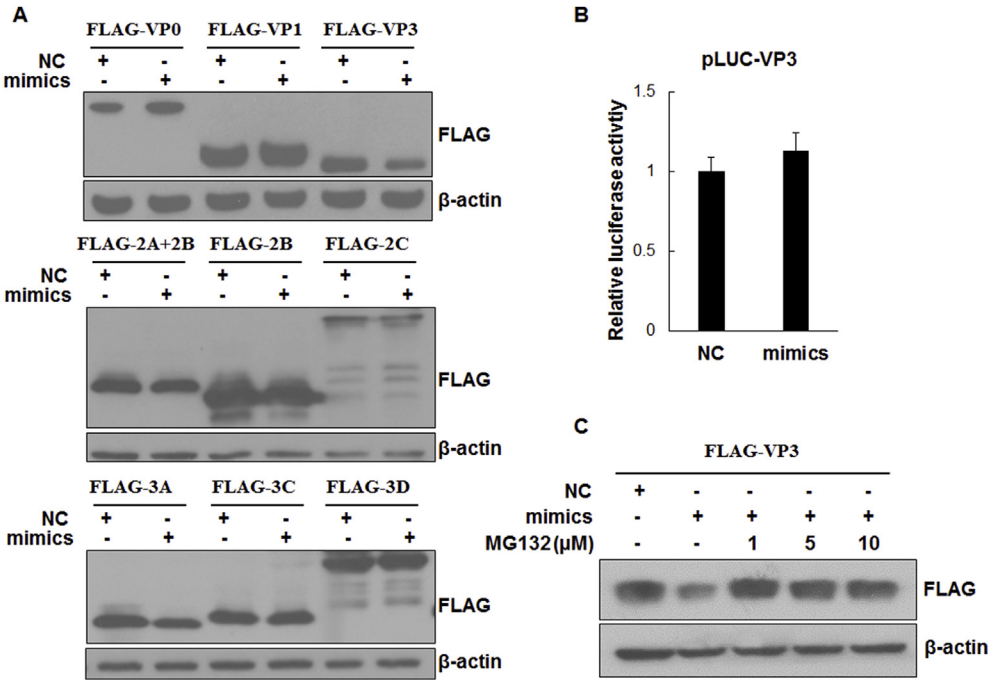

Fig. 4. MiR-1307 specifically promotes VP3 degradation indirectly through proteasome pathway.

(A) Co-transfection of miR-1307 mimics specifically reduces the protein expression of FLAG-VP3. BHK-21 cells were transfected with plasmids expressing FLAG-tagged different viral proteins together with miR-1307 mimics or scrambled negative-control (NC). Thirty-six hours after transfection, cells were collected for western blotting using antibodies against FLAG and β-actin. β-actin was used as the loading control. The experiment was repeated three times, yielding similar results.

(B) Co-transfection of miR-1307 mimics does not affect the relative luciferase activity of pLUC-VP3. BHK-21 cells in 24-well-plates were transfected with 200 ng of pLUC-VP3 together with 20 pmol of miR-1307 mimics or NC. Twenty-four hours after transfection, cells were lysed for measuring the relative luciferase activity. The experiments were performed in triplicates and the bars are SD. **(C)** MG132 treatment abolishes the reductive effects of miR-1307 on FLAG-VP3 protein expression. BHK-21 cells were transfected with pFLAG-VP3 together with NC or miR-1307 mimics. Twenty-four hours after transfection, cells were treated with increased amounts of MG132 or DMSO for another 12 h before being collected for western blotting. β-actin was used as the loading control. The experiment was repeated three times with similar result.

overexpression clones, and IFN-β whose expression was reduced. Collectively, these data demonstrated that overexpression of miR-1307 enhances the innate immune response. Transcription of type-I IFNs is dependent on coordinated activation of the latent transcription factors IRF-3 and NF-κB, through phosphorylation-dependent mechanisms (Kawai and Akira, 2006). To this end, we detected the abundance of these activated signaling molecules in the miR-1307-overexpressing cell clone after FMDV challenge over time. In the NC cells, the activated

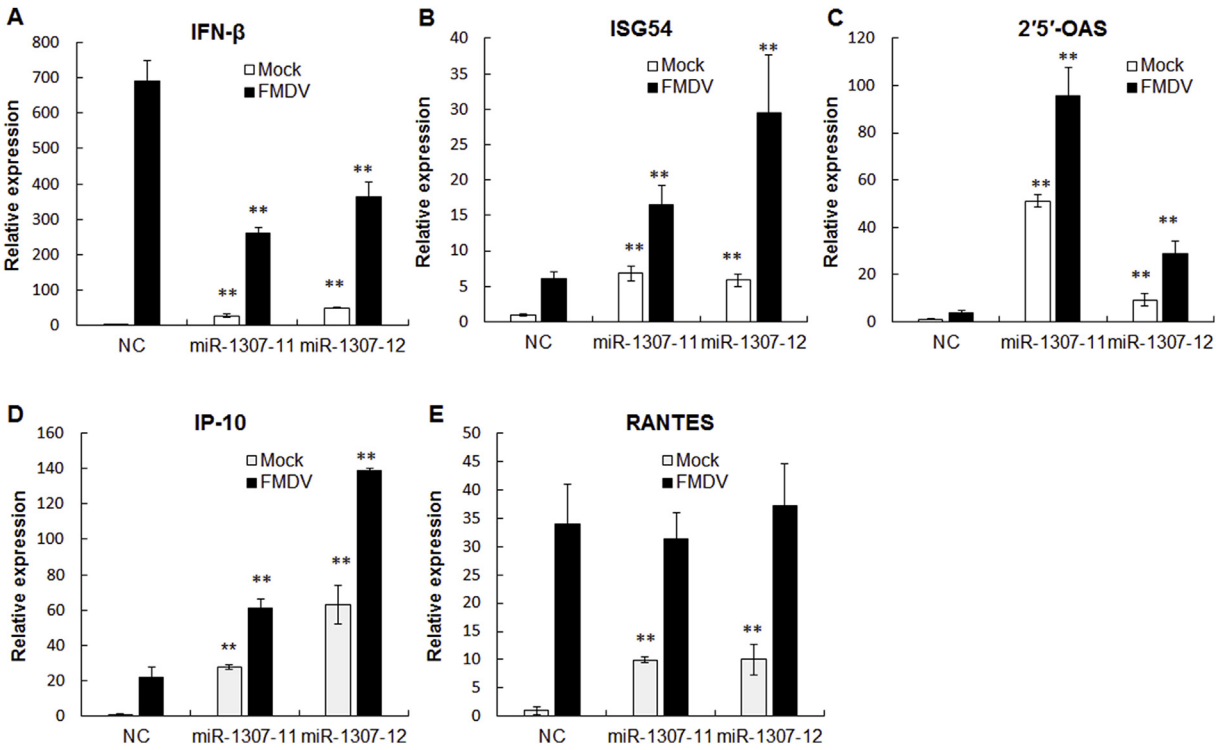

Fig. 5. Overexpression of miR-1307 enhances the expression of immune-responsive genes.

(A–E) Two independent PK-15 cell clones overexpressing miR-1307 and a control cell clone transformed with negative control plasmid (NC) were either mock-treated or infected with FMDV at 1 MOI. At 12 hpi, cells were collected for RNA extraction and RT-qPCR analysis. GAPDH was used as the internal control. The experiments were performed in triplicates and bars are SD. ** indicates significant differences at $p < 0.01$ according to Student's *t*-test, comparing to the corresponding value in NC.

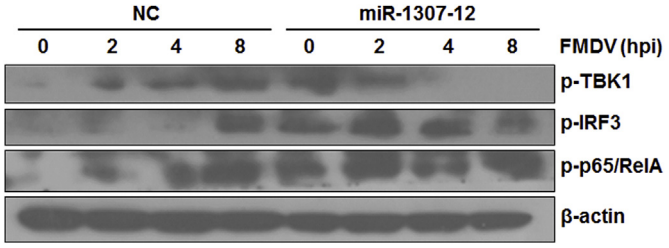

Fig. 6. Overexpression of miR-1307 activates the innate immune signaling. PK-15
cell clone overexpressing miR-1307 and a control cell clone (NC) were infected with 1 MOI of FMDV. At the indicated time points, cells were collected for western blotting experiments with the indicated antibodies. β-actin was used as the internal control. The experiments were repeated three times and similar results obtained.

molecules *p*-IRF3, NF-κB subunit p-p65/RelA, and *p*-TBK1 which is required for phosphorylation and activation of IRF3, were all barely detectable before FMDV infection. Upon viral challenge, these molecules gradually accumulated and reached maximum at 8 hpi. In comparison, in the miR-1307-12 cells, all of these proteins were already abundant without FMDV infection, indicating a pre-activated immune signaling. At 2 hpi and 4 hpi, the expression level of *p*-IRF3 and p-p65 was still significantly higher in the miR-1307-12 cells comparing with that in NC, while at 8 hpi, *p*-IRF3 and *p*-TBK1 were reduced (Fig. 6). Collectively, these data demonstrate that overexpression of miR-1307 pre-activates and enhances the innate immune signaling at the early infection stage and compromises it at the late stage.

3.6. Injection of miR-1307 agomir prolongs the lifespan of FMDV-infected suckling mice

Agomir and antagomir are chemically engineered oligonucleotides commonly used to mimic and inhibit miRNA function respectively in experimental animals. Therapeutic potential by manipulation of miRNAs with agomir/antagomir to control virus pathogens has been widely documented in literature (Laqtom and Buck, 2011; Tsunetsugu-Yokota and Yamamoto, 2010), especially for the liver-specific miR-122, antagomir of which has entered into human clinical trials to control HCV (Janssen et al., 2013; van der Ree et al., 2017). The obvious inhibitory effects of miR-1307 on FMDV replication prompted us to evaluate its therapeutic potential. Hence, we performed viral challenge assay in suckling mice, which have been widely used as animal models to study FMDV (Chen et al., 2004; Habiela et al., 2014). Three-day-old suckling mice (Balb/c) were subcutaneously inoculated in the neck with 100 LD_{50} of FMDV at 1 h after pre-injection of miR-1307 agomir or NC. Our preliminary test revealed that miR-1307 agomir could not be stable longer than 7 h in suckling mice (Fig. S5). Hence, at 12 hpi, NC or miR-1307 agomir was applied again with the same method. As can be clearly seen in Fig. 7, the mice from the NC group started to die at 28 hpi, while the first death of those from the agomir group occurred at 38 hpi. At 36 hpi, all of the mice from the NC group had died, but all from the agomir group were still alive at this time point and their lifespan was extended until 48 hpi, 12 h later than the control group (Fig. 7A). Together, this result demonstrated that miR-1307 significantly delays the FMDV-induced lethality in suckling mice. It has been documented that FMDV preferentially replicates in myocardium and death is often attributed to myocarditis (Habiela et al., 2014). Hence, we quantified the viral RNA abundance in heart tissues just before the death occurred (24 hpi). The result showed that FMDV RNA level was significantly reduced in the heart tissues from the agomir group mice (Fig. 7B), indicating application of miR-1307 agomir suppresses FMDV replication *in vivo*.

4. Discussion

MiRNAs as post-transcriptional regulators have been fully demonstrated to play important roles during various virus-host interplay through direct interaction with viral genome or regulation of host factors, exerting either proviral effects (Hou et al., 2009; Huang et al., 2016; Jopling et al., 2005; Scheel et al., 2016; Wu et al., 2013), or antiviral effects (Wang et al., 2012b; Wu et al., 2014; Zheng et al., 2013). In the case of FMDV, a number of miRNAs have been demonstrated to differentially express in PK-15 cells and also in bovine serum after FMDV infection (Basagoudanavar et al., 2018; Stenfeldt et al., 2017; Zhang et al., 2014). However, functional characterization and mechanistic study are still lacking, except miR-203a which has been shown to antagonize FMDV infection (Gutkoska et al., 2017). Here we expand the literature by demonstrating that porcine miR-1307 suppresses FMDV replication. Firstly, transient transfection of miR-1307 mimics significantly reduced the viral RNA in FMDV-infected cells, while transfection of its inhibitors slightly promoted FMDV replication (Fig. 2). Secondly, FMDV replication was also obviously attenuated in the cell lines stably overexpressing miR-1307 shown by RT-qPCR, western blotting and virus titration (Fig. 3). Lastly, injection of miR-1307 agomir significantly delayed the FMDV-induced lethality in suckling mice and reduced the viral RNA abundance in the heart tissues (Fig. 7). Together, these data prove that miR-1307 is a novel host miRNA that suppresses FMDV replication. The antiviral miR-1307 was rapidly induced upon FMDV challenge (Fig. 1), indicating it is part of host immune responses. It has been demonstrated that the Epstein Barr Virus (EBV)-mediated induction of miR-155 occurs through multiple processes involving cell signaling regulation, chromatin remodeling and transcription factor activation (Yin et al., 2016). However, the induction of miR-1307 occurred earlier than the full activation of the classical innate immune signaling components NF-κB and IRF 3/7. Hence, it would be interesting in the future to determine how the miR-1307 expression is stimulated upon FMDV infection.

Host miRNAs can suppress virus multiplication by directly blocking viral replication or targeting proviral host factors (Bruscella et al., 2017; Tsunetsugu-Yokota and Yamamoto, 2010). Targeting viral genome seems to be a more efficient and direct way to inhibit virus replication and the number of miRNAs reported to function through this mechanism has been growing (Pan et al., 2014; Wang et al., 2012b, 2017; Wen et al., 2015; Zheng et al., 2013). There are also some other documents that host miRNAs inhibit virus replication by suppressing proviral host factors (Santhakumar et al., 2010; Slonchak et al., 2015; Wu et al., 2014). Interestingly, miR-485 exhibited bispecificity, targeting host RIG-I in cells with a low abundance of H5N1 virus to prevent spurious activation of antiviral signaling and targeting viral PB1 in cells with increased amounts of the H5N1 virus to restrict virus infection (Ingle et al., 2015). Here we provide evidences demonstrating that the antiviral miR-1307 specifically promotes the degradation of FMDV structural protein VP3 indirectly through proteasome pathway. Co-transfection of miR-1307 mimics together with construct expressing different FLAG-tagged viral proteins showed that miR-1307 specifically reduced the protein expression of FLAG-VP3, but did not show any reproducible effects on the other viral proteins (Fig. 4A). Negative result from luciferase reporter assay excluded the possibility that miR-1307 directly target VP3 RNA (Fig. 4B). Further application of proteasome specific inhibitor MG132 completely abolished the inhibitory effects of miR-1307 on FLAG-VP3 protein expression (Fig. 4C), fully demonstrating that miR-1307 promotes VP3 degradation through proteasome pathway. Hence, it is possible that miR-1307 targets an unknown host factor required for VP3 protein stability.

The significant antiviral effects of miR-1307 prompted us to test its possible effects on the classical innate immune response. Our results showed that overexpression of miR-1307 pre-activates the expression of IFN-β and several ISGs, including ISG54, 2′,5′-OAS, IP-10 and RANTES before FMDV infection, and further enhances the expression of most of

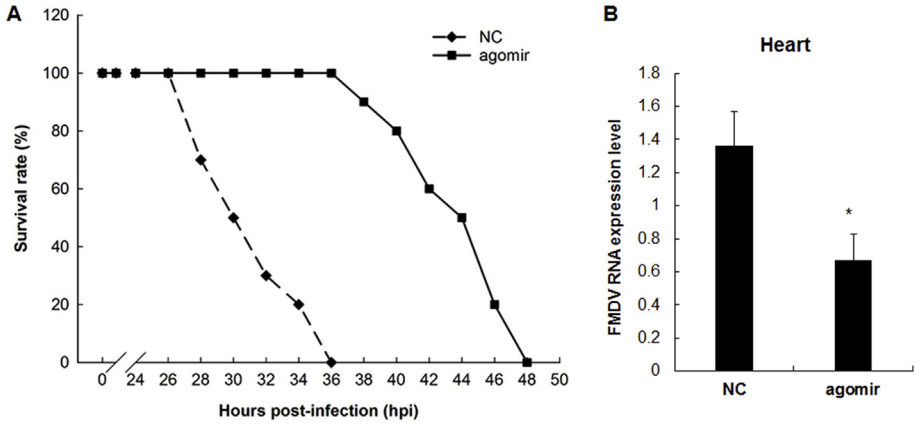

Fig. 7. Injection of miR-1307 agomir delays the FMDV-induced lethality in suckling mice.
(A) The survival rate of FMDV-infected suckling mice in the presence of NC or miR-1307 agomir. Three-day-old suckling mice were subcutaneously injected in the neck with 0.6 OD (100 μl) of NC or agomir at 1 h before they were challenged with FMDV (100 LD_{50}, 100 μl) with the same method. At 12 hpi, NC or agomir was applied again with the same method. The survival rate was calculated every 2 h until all the mice were dead. n = 10. The experiment was repeated three times and the similar result was obtained.
(B) FMDV replication was inhibited in the heart tissues of suckling mice applied with miR-1307 agomir. The experiment was performed the same as in (A). The mice were sentenced to death for the collection of heart tissues just before the FMDV-induced lethality occurs (24 hpi). Total RNA was extracted from the heart tissues and RT-qPCR targeting VP1 was performed to quantify FMDV RNA expression level. β-actin was used as the internal control. n = 5. Bars are SD and * indicates significant differences at $p < 0.05$ according to Student's *t*-test.

these genes after viral challenge (Fig. 5). Consistently, accumulation of the activated *p*-TBK1, *p*-IRF3 and p-p65 was abundant in the miR-1307-overexpressing cells without FMDV infection, and expression of *p*-IRF3 and p-p65 remained higher at the early stage of infection (Fig. 6). Together, these data demonstrate that miR-1307 activates the immune signaling and enhances the immune response. The reduction of IFN-β at 12 hpi and the decrease of *p*-TBK1, *p*-IRF3 at the late stage of infection in the miR-1307-overexpressing cells might be due to the dramatically reduced stimuli (FMDV RNA) in these cells, and/or a negative feedback mechanism to prevent the over-activation of the immune response.

At the moment, degradation of VP3 and enhancement of immune response seem to be two independent effects of miR-1307. However, we cannot exclude the possibility that both of them are caused by the knock-down of a common target by miR-1307. Actually, according to a recent progress in one of our colleagues Haixue Zheng's group, overexpression of TBK1 promotes the ubiquitination and proteasome degradation of VP3 (unpublished, being reviewed). In our result, *p*-TBK1 was highly enriched in miR-1307-overexpressing cells. Hence, it is possible that miR-1307 targets a TBK1 negative regulator, and the accumulation of TBK1 causes both the degradation of VP3 and the enhancement of immune response.

We tried to identify the direct target of miR-1307 responsible, but the attempts by now were unsuccessful. We predicted the possible targets of miR-1307 in PK-15 cells using the miRanda algorithm (John et al., 2004). The predicted targets were then used as input for KEGG pathway analysis. As shown in Fig. S6, ubiquitin mediated proteolysis and RIG-I-like receptor signaling pathway are the two most highly enriched pathways, which seem to be closely related to the biological function of miR-1307. However, when we tested them in luciferase reporter assay, none of them were genuine target (Fig. S7). We then tried to predict its potential targets using three well-used algorithms, including miRanda (John et al., 2004), PITA (Kertesz et al., 2007) and TargetScan (Lewis et al., 2005). The intersections of the prediction results are shown in Fig. S8 and those potential targets shared by at least two algorithms are listed in Table S2, for reference in future study. Hopefully, UV cross-linking and immunoprecipitation (CLIP) using AGO specific antibodies can be used to experimentally identify the AGO bound transcriptomes which are possibly targeted by miRNAs. Recently, AGO CLIP-seq data has been integrated with bioinformatics algorithm to significantly increase the accuracy of miRNA targets prediction in human and mouse (Ahadi et al., 2017; Li et al., 2014). However, the lack of AGO CLIP-seq data in porcine samples limit the accuracy of the current miRNA target prediction methods. Further investigation with AGO CLIP in PK-15 cells will be helpful to identify the direct targets of miR-1307 and understand the roles of miRNAs during FMDV-host interaction from a whole-scale view.

FMD is a highly contagious viral disease of cloven-hoofed animals. Currently, vaccination is known to be the most effective measure in preventing FMD. However, it has been shown that production of immune antibodies against FMD reached maximum two weeks after the vaccinations in cattle and in pigs four weeks after the vaccinations (Park, 2013), while FMDV can replicates and spreads extremely rapidly, causing the appearance of clinical syndrome as early as 2–3 days post-infection. The delayed immune response necessitate other relatively rapid control strategies as well as the long-lasting vaccination approaches during FMD outbreak (Grubman and de los Santos, 2005). The artificially designed miRNAs targeting the viral genome have shown their potential in repressing FMDV replication (Chang et al., 2013; Du et al., 2011), and it has been proposed that administration of siRNA in combination of vaccines can potentially be more effective (Grubman and de los Santos, 2005). The host miRNA miR-1307 identified here can significantly prolong the lifespan of FMDV-infected suckling mice. Moreover, more robust protective effects hopefully expected from the future experimental study in mice and/or pigs when the chemically stabilized agomir was applied with the help of a delivery vehicle (i.e. Invivofectamine), together with cost reduction of agomir biosynthesis in future, may facilitate miR-1307 to be a potential candidate to serve this purpose.

Conflicts of interest

The authors declare no conflicts of interests.

Acknowledgment

This research was financially supported by the grants from Central Public-interest Scientific Institution Basal Research Fund (1610312016010), National Key R&D Program of China (2016YFD0501500), National Natural Science Foundation of China (31672538) and China Agricultural Research System (CARS-35). We appreciate Dr. Haixue Zheng for providing the *anti*-VP1 antibody.

Appendix A. Supplementary data

Supplementary data to this article can be found online at https://doi.org/10.1016/j.virol.2019.07.009.

References

Ahadi, A., Sablok, G., Hutvagner, G., 2017. miRTar2GO: a novel rule-based model learning method for cell line specific microRNA target prediction that integrates Ago2 CLIP-Seq and validated microRNA-target interaction data. Nucleic Acids Res. 45, e42.
Bachrach, H.L., 1968. Foot-and-mouth disease. Annu. Rev. Microbiol. 22, 201–244.

Basagoudanavar, S.H., Hosamani, M., Tamil Selvan, R.P., Sreenivasa, B.P., Sanyal, A., Venkataramanan, R., 2018. Host serum microRNA profiling during the early stage of foot-and-mouth disease virus infection. Arch. Virol. 163, 2055–2063.
Browne, E.P., Li, J., Chong, M., Littman, D.R., 2005. Virus-host interactions: new insights from the small RNA world. Genome Biol. 6, 238.
Bruscella, P., Bottini, S., Baudesson, C., Pawlotsky, J.M., Feray, C., Trabucchi, M., 2017. Viruses and miRNAs: more friends than foes. Front. Microbiol. 8, 824.
Chang, Y., Dou, Y., Bao, H., Luo, X., Liu, X., Mu, K., Liu, Z., Liu, X., Cai, X., 2013. Multiple microRNAs targeted to internal ribosome entry site against foot-and-mouth disease virus infection *in vitro* and *in vivo*. Virol. J. 11, 1–12.
Chen, W., Yan, W., Du, Q., Fei, L., Liu, M., Ni, Z., Sheng, Z., Zheng, Z., 2004. RNA interference targeting VP1 inhibits foot-and-mouth disease virus replication in BHK-21 cells and suckling mice. J. Virol. 78, 6900–6907.
de Los Santos, T., Diaz-San Segundo, F., Grubman, M.J., 2007. Degradation of nuclear factor kappa B during foot-and-mouth disease virus infection. J. Virol. 81, 12803–12815.
Deddouche, S., Goubau, D., Rehwinkel, J., Chakravarty, P., Begum, S., Maillard, P.V., Borg, A., Matthews, N., Feng, Q., van Kuppeveld, F.J., Reis e Sousa, C., 2014. Identification of an LGP2-associated MDA5 agonist in picornavirus-infected cells. Elife 3, e01535.
Domingo, E., Baranowski, E., Escarmis, C., Sobrino, F., 2002. Foot-and-mouth disease virus. Comp. Immunol. Microbiol. Infect. Dis. 25, 297–308.
Domingo, E., Pariente, N., Airaksinen, A., Gonzalez-Lopez, C., Sierra, S., Herrera, M., Grande-Perez, A., Lowenstein, P.R., Manrubia, S.C., Lazaro, E., Escarmis, C., 2005. Foot-and-mouth disease virus evolution: exploring pathways towards virus extinction. Curr. Top. Microbiol. Immunol. 288, 149–173.
Du, J., Gao, S., Luo, J., Zhang, G., Cong, G., Shao, J., Lin, T., Cai, X., Chang, H., 2011. Effective inhibition of foot-and-mouth disease virus (FMDV) replication *in vitro* by vector-delivered microRNAs targeting the 3D gene. Virol. J. 8, 292.
Du, Y., Bi, J., Liu, J., Liu, X., Wu, X., Jiang, P., Yoo, D., Zhang, Y., Wu, J., Wan, R., Zhao, X., Guo, L., Sun, W., Cong, X., Chen, L., Wang, J., 2014. 3Cpro of foot-and-mouth disease virus antagonizes the interferon signaling pathway by blocking STAT1/STAT2 nuclear translocation. J. Virol. 88, 4908–4920.
Feng, Q., Hato, S.V., Langereis, M.A., Zoll, J., Virgen-Slane, R., Peisley, A., Hur, S., Semler, B.L., van Rij, R.P., van Kuppeveld, F.J., 2012. MDA5 detects the double-stranded RNA replicative form in picornavirus-infected cells. Cell Rep. 2, 1187–1196.
Gao, Y., Sun, S.Q., Guo, H.C., 2016. Biological function of Foot-and-mouth disease virus non-structural proteins and non-coding elements. Virol. J. 13, 107.
Grubman, M.J., de los Santos, T., 2005. Rapid control of foot-and-mouth disease outbreaks: is RNAi a possible solution? Trends Immunol. 26, 65–68.
Guarne, A., Tormo, J., Kirchweger, R., Pfistermueller, D., Fita, I., Skern, T., 1998. Structure of the foot-and-mouth disease virus leader protease: a papain-like fold adapted for self-processing and eIF4G recognition. EMBO J. 17, 7469–7479.
Gutkoska, J., LaRocco, M., Ramirez-Medina, E., de Los Santos, T., Lawrence, P., 2017. Host microRNA-203a is antagonistic to the progression of foot-and-mouth disease virus infection. Virology 504, 52–62.
Habiela, M., Seago, J., Perez-Martin, E., Waters, R., Windsor, M., Salguero, F.J., Wood, J., Charleston, B., Juleff, N., 2014. Laboratory animal models to study foot-and-mouth disease: a review with emphasis on natural and vaccine-induced immunity. J. Gen. Virol. 95, 2329–2345.
Hou, J., Wang, P., Lin, L., Liu, X., Ma, F., An, H., Wang, Z., Cao, X., 2009. MicroRNA-146a feedback inhibits RIG-I-dependent type I IFN production in macrophages by targeting TRAF6, IRAK1, and IRAK2. J. Immunol. 183, 2150–2158.
Huang, Y., Wang, W., Ren, Q., 2016. Two host microRNAs influence WSSV replication via STAT gene regulation. Sci. Rep. 6, 23643.
Huntzinger, E., Izaurralde, E., 2011. Gene silencing by microRNAs: contributions of translational repression and mRNA decay. Nat. Rev. Genet. 12, 99–110.
Ingle, H., Kumar, S., Raut, A.A., Mishra, A., Kulkarni, D.D., Kameyama, T., Takaoka, A., Akira, S., Kumar, H., 2015. The microRNA miR-485 targets host and influenza virus transcripts to regulate antiviral immunity and restrict viral replication. Sci. Signal. 8, ra126.
Janssen, H.L., Reesink, H.W., Lawitz, E.J., Zeuzem, S., Rodriguez-Torres, M., Patel, K., van der Meer, A.J., Patick, A.K., Chen, A., Zhou, Y., Persson, R., King, B.D., Kauppinen, S., Levin, A.A., Hodges, M.R., 2013. Treatment of HCV infection by targeting microRNA. N. Engl. J. Med. 368, 1685–1694.
John, B., Enright, A.J., Aravin, A., Tuschl, T., Sander, C., Marks, D.S., 2004. Human microRNA targets. PLoS Biol. 2, e363.
Jopling, C.L., Yi, M., Lancaster, A.M., Lemon, S.M., Sarnow, P., 2005. Modulation of hepatitis C virus RNA abundance by a liver-specific MicroRNA. Science 309, 1577–1581.
Kawai, T., Akira, S., 2006. Innate immune recognition of viral infection. Nat. Immunol. 7, 131–137.
Kertesz, M., Iovino, N., Unnerstall, U., Gaul, U., Segal, E., 2007. The role of site accessibility in microRNA target recognition. Nat. Genet. 39, 1278–1284.
Krol, J., Loedige, I., Filipowicz, W., 2010. The widespread regulation of microRNA biogenesis, function and decay. Nat. Rev. Genet. 11, 597–610.
Laqtom, N.N., Buck, A.H., 2011. MicroRNA manipulation as a host-targeted antiviral therapeutic strategy. Eur. Pharm. Rev. 16, 52–55.
Lewis, B.P., Burge, C.B., Bartel, D.P., 2005. Conserved seed pairing, often flanked by adenosines, indicates that thousands of human genes are microRNA targets. Cell 120, 15–20.
Li, J., Wei, H., Li, Y., Li, Q., Li, N., 2012. Identification of a suitable endogenous control gene in porcine blastocysts for use in quantitative PCR analysis of microRNAs. Sci. China Life Sci. 55, 126–131.
Li, J.H., Liu, S., Zhou, H., Qu, L.H., Yang, J.H., 2014. starBase v2.0: decoding miRNA-ceRNA, miRNA-ncRNA and protein-RNA interaction networks from large-scale CLIP-Seq data. Nucleic Acids Res. 42, D92–D97.
Pan, D., Flores, O., Umbach, J.L., Pesola, J.M., Bentley, P., Rosato, P.C., Leib, D.A., Cullen, B.R., Coen, D.M., 2014. A neuron-specific host microRNA targets herpes simplex virus-1 ICP0 expression and promotes latency. Cell Host Microbe 15, 446–456.
Park, J.H., 2013. Requirements for improved vaccines against foot-and-mouth disease epidemics. Clin. Exp. Vaccine Res. 2, 8–18.
Santhakumar, D., Forster, T., Laqtom, N.N., Fragkoudis, R., Dickinson, P., Abreu-Goodger, C., Manakov, S.A., Choudhury, N.R., Griffiths, S.J., Vermeulen, A., Enright, A.J., Dutia, B., Kohl, A., Ghazal, P., Buck, A.H., 2010. Combined agonist-antagonist genome-wide functional screening identifies broadly active antiviral microRNAs. Proc. Natl. Acad. Sci. U. S. A. 107, 13830–13835.
Scheel, T.K., Luna, J.M., Liniger, M., Nishiuchi, E., Rozen-Gagnon, K., Shlomai, A., Auray, G., Gerber, M., Fak, J., Keller, I., Bruggmann, R., Darnell, R.B., Ruggli, N., Rice, C.M., 2016. A broad RNA virus survey reveals both miRNA dependence and functional sequestration. Cell Host Microbe 19, 409–423.
Slonchak, A., Shannon, R.P., Pali, G., Khromykh, A.A., 2015. Human microRNA miR-532-5p exhibits antiviral activity against west nile virus via suppression of host genes SESTD1 and TAB3 required for virus replication. J. Virol. 90, 2388–2402.
Sobrino, F., Saiz, M., Jimenez-Clavero, M.A., Nunez, J.I., Rosas, M.F., Baranowski, E., Ley, V., 2001. Foot-and-mouth disease virus: a long known virus, but a current threat. Vet. Res. 32, 1–30.
Stenfeldt, C., Arzt, J., Smoliga, G., LaRocco, M., Gutkoska, J., Lawrence, P., 2017. Proof-of-concept study: profile of circulating microRNAs in bovine serum harvested during acute and persistent FMDV infection. Virol. J. 14, 71.
Sun, Y., Kasiappan, R., Tang, J., Webb, P.L., Quarni, W., Zhang, X., Bai, W., 2014. A novel function of the Fe65 neuronal adaptor in estrogen receptor action in breast cancer cells. J. Biol. Chem. 289, 12217–12231.
Tsunetsugu-Yokota, Y., Yamamoto, T., 2010. Mammalian microRNAs: post-transcriptional gene regulation in RNA virus infection and therapeutic applications. Front. Microbiol. 1, 108.
van der Ree, M.H., de Vree, J.M., Stelma, F., Willemse, S., van der Valk, M., Rietdijk, S., Molenkamp, R., Schinkel, J., van Nuenen, A.C., Beuers, U., Hadi, S., Harbers, M., van der Veer, E., Liu, K., Grundy, J., Patick, A.K., Pavlicek, A., Blem, J., Huang, M., Grint, P., Neben, S., Gibson, N.W., Kootstra, N.A., Reesink, H.W., 2017. Safety, tolerability, and antiviral effect of RG-101 in patients with chronic hepatitis C: a phase 1B, double-blind, randomised controlled trial. Lancet 389, 709–717.
Wang, D., Fang, L., Li, K., Zhong, H., Fan, J., Ouyang, C., Zhang, H., Duan, E., Luo, R., Zhang, Z., Liu, X., Chen, H., Xiao, S., 2012a. Foot-and-mouth disease virus 3C protease cleaves NEMO to impair innate immune signaling. J. Virol. 86, 9311–9322.
Wang, D., Fang, L., Li, P., Sun, L., Fan, J., Zhang, Q., Luo, R., Liu, X., Li, K., Chen, H., Chen, Z., Xiao, S., 2011. The leader proteinase of foot-and-mouth disease virus negatively regulates the type I interferon pathway by acting as a viral deubiquitinase. J. Virol. 85, 3758–3766.
Wang, L., Qin, Y., Tong, L., Wu, S., Wang, Q., Jiao, Q., Guo, Z., Lin, L., Wang, R., Zhao, W., Zhong, Z., 2012b. MiR-342-5p suppresses coxsackievirus B3 biosynthesis by targeting the 2C-coding region. Antivir. Res. 93, 270–279.
Wang, R., Zhang, Y.Y., Lu, J.S., Xia, B.H., Yang, Z.X., Zhu, X.D., Zhou, X.W., Huang, P.T., 2017. The highly pathogenic H5N1 influenza A virus down-regulated several cellular MicroRNAs which target viral genome. J. Cell Mol. Med. 21, 3076–3086.
Wen, W., He, Z., Jing, Q., Hu, Y., Lin, C., Zhou, R., Wang, X., Su, Y., Yuan, J., Chen, Z., Yuan, J., Wu, J., Li, J., Zhu, X., Li, M., 2015. Cellular microRNA-miR-548g-3p modulates the replication of dengue virus. J. Infect. 70, 631–640.
Wu, N., Gao, N., Fan, D., Wei, J., Zhang, J., An, J., 2014. miR-223 inhibits dengue virus replication by negatively regulating the microtubule-destabilizing protein STMN1 in EAhy926 cells. Microb. Infect. 16, 911–922.
Wu, S., He, L., Li, Y., Wang, T., Feng, L., Jiang, L., Zhang, P., Huang, X., 2013. miR-146a facilitates replication of dengue virus by dampening interferon induction by targeting TRAF6. J. Infect. 67, 329–341.
Yin, Q., Wang, X., Roberts, C., Flemington, E.K., Lasky, J.A., 2016. Methylation status and AP1 elements are involved in EBV-mediated miR-155 expression in EBV positive lymphoma cells. Virology 494, 158–167.
Zhang, K.S., Liu, Y.J., Kong, H.J., Cheng, W.W., Shang, Y.J., Tian, H., Zheng, H.X., Guo, J.H., Liu, X.T., 2014. Identification and analysis of differential miRNAs in PK-15 cells after foot-and-mouth disease virus infection. PLoS One 9, e90865.
Zheng, Z., Ke, X., Wang, M., He, S., Li, Q., Zheng, C., Zhang, Z., Liu, Y., Wang, H., 2013. Human microRNA hsa-miR-296-5p suppresses enterovirus 71 replication by targeting the viral genome. J. Virol. 87, 5645–5656.
Zhu, Z., Wang, G., Yang, F., Cao, W., Mao, R., Du, X., Zhang, X., Li, C., Li, D., Zhang, K., Shu, H., Liu, X., Zheng, H., 2016. Foot-and-mouth disease virus viroporin 2B antagonizes RIG-I-mediated antiviral effects by inhibition of its protein expression. J. Virol. 90, 11106–11121.